



Ascorbic acid-loaded poly(lactic-co-glycolic acid) nanoparticles incorporated into a polyacrylic acid gel as a promising tool for site-specific oral cancer therapy

Nurul Ain Mohammad Hamdi¹, Ahmad Fahmi Harun Ismail²,
Muhammad Salahuddin Haris¹, Widya Lestari³

¹Department of Pharmaceutical Technology, Kulliyah of Pharmacy, International Islamic University Malaysia, Kuantan, Pahang, Malaysia, ²Department of Physical Rehabilitation Sciences, Kulliyah of Allied Health Sciences, International Islamic University Malaysia, Kuantan, Pahang, Malaysia, ³Department of Oral Biology, Kulliyah of Dentistry, International Islamic University Malaysia, Kuantan, Pahang, Malaysia

Corresponding Author:

Nurul Ain binti Mohammad Hamdi, Kulliyah of Pharmacy, International Islamic University Malaysia, Kuantan, Pahang, Malaysia.
E-mail: aenhamdi@gmail.com

Received: September 10, 2021

Accepted: March 08, 2022

Published: January 16, 2023

ABSTRACT

Background: Chemotherapy is commonly used in oral cancer therapy, especially as the disease advances. However, it is associated with terrible adverse effects and the occurrence of chemoresistance which causes treatment failure. Thus, discovering a new potential anticancer agent and developing a safe, effective, and non-invasive drug delivery are necessary. **Objective:** The objective of the current study is to develop ascorbic acid-loaded poly(lactic-co-glycolic) acid (AA-PLGA) nanoparticles incorporated into polyacrylic acid gel intended to treat oral cancer. **Materials and methods:** Double emulsion solvent evaporation method was used to fabricate AA-PLGA nanoparticles. Optimization was carried out in the primary emulsion based on multilevel factorial design by testing at varying surfactant types and concentrations. The optimized nanoparticles formulation was further incorporated into different concentrations of polyacrylic acid gel, and compared with a mucoadhesive polyacrylic acid-based commercial product (Kin Care) as a reference. The optimized AA-PLGA nanoparticles were subjected to cytotoxic assay against the SCC-25 cell line. **Results:** For the optimized formulation, we observed particle size of 252 ± 2.98 nm, polydispersity index (PDI) of 0.151 ± 0.02 , zeta potential of -20.93 ± 0.87 mV, and encapsulation efficiency of $69.73 \pm 1.07\%$. Polyacrylic acid polymer with a strength of 1% was chosen as the optimum gelling agent for AA-PLGA nanoparticles-in-gel formulation. Cytotoxicity study of the optimized nanoparticle demonstrated significant ($P < 0.05$) reduction of cancer cell viability in a dose-dependent manner with a half-maximal inhibitory concentration value of 2.42 mg/mL. **Conclusion:** The results of the present study support the feasibility of AA-PLGA nanoparticles-in-gel formulation for oral cancer therapy.

Keywords: Anti-cancer, ascorbic acid, mucoadhesive gel, nanoparticles, oral cancer, PLGA

INTRODUCTION

Oral cancer accounts for 377, 713 new cases and 177, 757 deaths in 2020, making it the seventeenth most common cancer worldwide.^[1] It is associated with significant mortality, especially if the patient is diagnosed at an advanced stage.^[2] Often, chemotherapy is required in the late-stage as well as in metastatic oral cancer.^[3] However,

conventional chemotherapy approaches are associated with several disadvantages, particularly the terrible adverse effects to the patient and occurrence of chemoresistance toward commonly used chemotherapy which accounts for the treatment failure, disease recurrence, and metastasis.^[4-6] Hence, identifying a new potential anticancer agent and developing a safe, effective, and non-invasive drug delivery are necessary for complementary or alternative oral cancer therapy.

High dose (millimolar concentration) of ascorbic acid has been shown to be cytotoxic against oral cancer cells.^[7-9] However, formulating ascorbic acid is difficult due to its instability in the bulk aqueous system.^[10] Several approaches have been adopted to preserve its stability and enhance its delivery to the target site, such as formulation of multiple emulsion, and microparticles including nanoparticles.^[10-12] Furthermore, nanoparticulate systems have been reported to improve drug accumulation, drug uptake, and drug absorption across biological barriers.^[13,14]

Poly(lactic-co-glycolic acid) (PLGA) is a biodegradable synthetic hydrophobic polymer frequently employed to develop various therapeutic devices including drug delivery systems.^[15,16] Double emulsion solvent evaporation is a method to prepare PLGA-based microparticles and nanoparticles.^[17,18] Many active pharmaceutical agents have been successfully encapsulated in PLGA through this method.^[18-21] The primary advantage of this method is the ability to encapsulate both lipophilic and hydrophilic drugs.^[22] This technique involves two steps of emulsification: First emulsification produces a primary emulsion (water-in-oil) and the second emulsification produces a secondary emulsion (water-in-oil-in-water). The hydrophilic drug is incorporated in the inner aqueous phase (W1). Meanwhile, the biodegradable polymer is incorporated in the oil phase (O) containing an organic solvent. Later, both phases are homogenized through proper agitation either with a homogenizer or sonicator to form a primary emulsion (W1/O). The primary emulsion is further emulsified with an external aqueous phase (W2) to form a secondary emulsion (W1/O/W2). Incorporation of appropriate surfactant in both emulsions is needed to stabilize the emulsion.^[23] For example, emulsifier with hydrophilic-lipophilic balance (HLB) value in the range of 3.5–8 is commonly used to stabilize water-in-oil emulsion (W/O). Meanwhile, polyvinyl alcohol (PVA) which possesses a high HLB (18) value is frequently used as the surfactant of choice for the production of secondary emulsion.^[24] HLB is an indicator of the solubilizing properties of emulsifiers, indicating the best type of emulsion to use either water-in-oil or oil-in-water emulsion.^[25]

Local drug delivery using high dose ascorbic acid directly to the cancerous site is favorable due to its non-invasive and straightforward.^[26] It is considered a safe and non-invasive strategy for treating oral tumors.^[27] However, since oral squamous cell carcinoma affects the epithelial themselves, site-specific targeting drugs need to penetrate and retain within the epithelium for optimum treatment.^[28] Besides that, easy access to the affected area and clear visibility of the oral cavity has made local intraoral delivery an attractive route for chemopreventive agents to the target site.^[29] With this approach, the systemic adverse effects of cytotoxic agents can be reduced due to the lesser extent of systemic drug absorption.^[26]

The pH of saliva, residence time of the formulation, salivary washout, and swallowing are the factors that need to be considered in a pharmaceutical formulation for topical oral application.^[30] The primary strategy of overcoming the low residence of formulation on the application site is through the incorporation of a mucoadhesive constituent to the conventional

dosage form.^[31] Polyacrylic acid is a mucoadhesive polymer that is widely studied for topical delivery of pharmaceutical agents to the mucous membrane.^[32-35] Its desirable properties, which are biodegradable, bioadhesive, non-irritant, not absorbed into the body and above all, economical, have made polyacrylic acid a frequently used gelling agent for topical application.^[35,36] Thus, this present study aims to develop ascorbic acid-loaded poly(lactic-co-glycolic) acid (AA-PLGA) nanoparticles to harness the aforementioned advantages, and to further incorporate them into polyacrylic acid gel for topical application on the oral mucosa.

MATERIALS AND METHODS

Materials

Ascorbic acid powder (purity 99.7%) was purchased from Thermo Fisher Scientific, Merelbeke Belgium. Triethanolamine was purchased from Fisher Scientific (M), Selangor, Malaysia. Span 20, Span 40, Span 80, and fetal bovine serum (FBS) were purchased from Sigma-Aldrich, Missouri, USA. PVA with (the polymer molecular weight of approximately 84,000 Mn and polyacrylic acid (Carbopol® 940) were purchased from EvaChem, Selangor, Malaysia. Kin Care oral gel Laboratorios KIN (Barcelona, Spain) was purchased from a community pharmacy in Kuantan, Pahang, Malaysia. Cellulose acetate membrane was purchased from Sartorius AG, Gottingen, Germany. PLGA with a viscosity of 0.4 dL/g (34 kDa) was purchased from Corbion, Amsterdam, Netherland. Chloroform, denatured ethanol (95%) and dimethyl sulfoxide were purchased from Merck Millipore, Darmstadt, Germany. Phosphate-buffered saline (PBS) was acquired from Invitrogen, Maryland, USA. SCC-25 cell line (ATCC®CRL-1628) was purchased from the American Type Culture Collection (ATCC), Virginia, USA. Dulbecco's modified Eagle's medium (DMEM), Penicillin-streptomycin, Trypan blue, and 3-(4,5-dimethylthiazol-2-yl)-2,5-diphenyl tetrazolium bromide (MTT) powder were purchased from Gibco, Maryland, USA. Trypsin was purchased from Thermo Fisher Scientific, Massachusetts, USA.

Preparation and Characterization of Nanoparticles

Fabrication of AA-PLGA nanoparticles

AA-PLGA nanoparticles were prepared using a double emulsion solvent evaporation technique with PLGA/ascorbic acid ratio of 1:1 w/w. The double emulsion solvent evaporation method was adapted and modified from an established method.^[18] Briefly, 100 mg of PLGA was dissolved in 3 mL of chloroform as organic solvent (oil phase). Different low HLB value surfactants with various concentrations were added into the oil phase and were regarded as the manipulated variable. Volume of 400 µL of aqueous phase containing 100 mg of ascorbic acid dissolved in distilled water was emulsified with the organic solvent with an ultra sonicator (QSonica, Connecticut, USA) for 4 min and 30 s at 80% amplitude under an ice bath to form a primary emulsion. The secondary emulsion was achieved by sonication between primary emulsion with 10 mL of 1% w/v PVA solution with the ultra sonicator for 4 min and 30 s at 80% amplitude under an ice bath. Then, the double emulsion was transferred into a

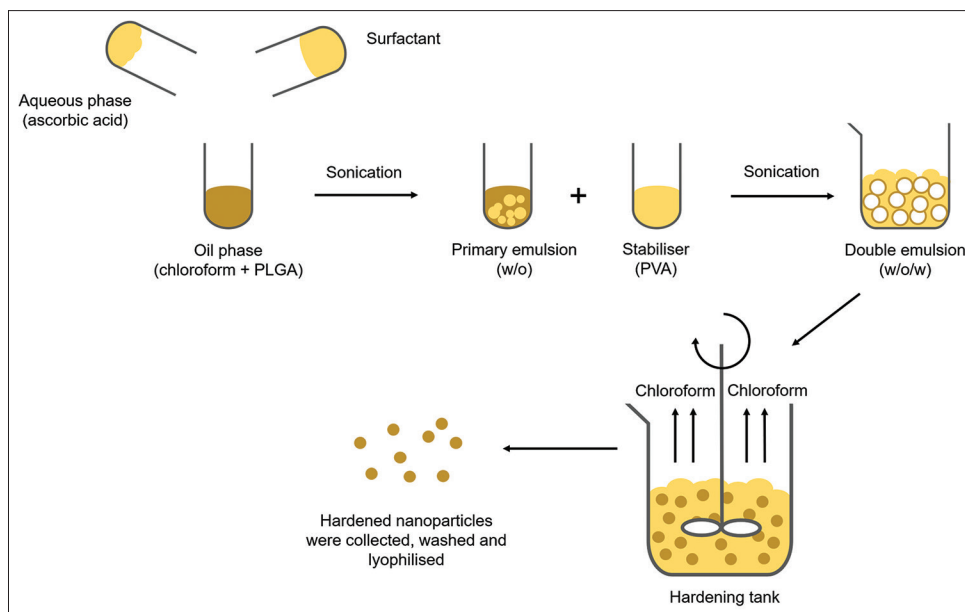


Figure 1: Steps of ascorbic acid-poly(lactic-co-glycolic) acid nanoparticles preparation through a double emulsion solvent evaporation method

hardening tank (20 mL of 1% w/v PVA solution with the high-speed stirring condition) for the solvent evaporation process which took 3 h. The steps of the nanoparticle's preparation are summarized in Figure 1. The nanoparticles were collected through centrifugation (4000 rev/min, 20 min) with Supra 22K high-speed centrifuge (Hanil, Gimpo, South Korea) and followed by washing with distilled water to remove PVA residual. The nanoparticles were freeze-dried for 24 h.

Experimental design and analysis

A multilevel categorical full factorial design was performed using Design-Expert Software (Minnesota, USA) to determine the effect of different experimental factors on the PLGA nanoparticle characteristics. The type of Span surfactant and concentration used in the primary emulsion was chosen as the factor of interest [Table 1]. The dependent variables were particle size, PDI, zeta potential, and encapsulation efficiency. For the experimental design, 12 formulations were prepared and the outline of the experimental plan and its result is presented in Table 2.

Measurement of particle size, PDI and zeta potential

PDI was evaluated to measure the degree of non-uniformity of the size distribution.^[37] The average particle size and PDI measurement were evaluated using Nano S (Malvern Zetasizer, Malvern, United Kingdom). Zeta potential measures the electric charge on the surface of the nanoparticles.^[38] Zeta potential can be positive or negative depending on the nature of the polymer used.^[39] Zeta potential measurement was evaluated using Nano Z (Malvern Zetasizer, Malvern, United Kingdom). All the samples were run in triplicate. Freshly prepared nanoparticles (0.2 mL) were suspended in 6 mL of distilled water before being subjected for measurement.

Determination of encapsulation efficiency

Nanoparticles (10 mg) were placed in a 2 mL microcentrifuge tube and re-dissolved using 1 mL of chloroform and 1 mL of

Table 1: Process and formulation parameter of the multilevel categorical full factorial

Code	Component	Unit	Level/category			
A	Span surfactant type	-	20	40	80	
B	Surfactant concentration	%	1	2	3	4

distilled water. The tube was rotated end-to-end for 1 h before it was subjected to the centrifugation process (5000 rev/min, 5 min) with Mikro 120 (Hettich centrifuge, Westphalia, Germany). Next, 20 μ L of the upper part of the sample (distilled water) were transferred into a 10 mL volumetric flask and distilled water was added to the 10 mL mark. The sample containing encapsulated ascorbic acid (2 mL) was subjected to a UV-visible spectrophotometer (Shimadzu, Kyoto, Japan). The absorbance was measured using a UV-visible spectrophotometer at a wavelength of 266 nm for ascorbic acid. The analytical method of quantification of ascorbic acid in PLGA nanoparticles was developed and validated as per ICH Topic Q2 (R1) guidelines.^[40] The measurement was done in triplicate and the average, as well as the standard error, was calculated. The percentage of encapsulation efficiency tells the percentage of ascorbic acid successfully encapsulated in the PLGA nanoparticles.^[41] (W_1) weight of ascorbic acid in nanoparticles and (W_2) The initial weight of ascorbic acid added. It was calculated using the following equation.

$$\text{Encapsulation efficiency} = W_1/W_2 \times 100$$

Scanning electron microscopic (SEM) analysis

SEM is conducted to characterize and visualize the shape and size distribution of nanoparticles. The external morphology of the nanoparticles was evaluated by using a Quanta 340 (FEI, Oregon, USA). Lyophilized nanoparticles were placed on an aluminum stud and coated with gold.

Table 2: Outline of the experimental design and results

Formulation	Independent variables		Measured dependent variables			
	Span surfactant type	Surfactant concentration %	Particle size (nm)	Polydispersity index	Zeta potential (mV)	Encapsulation efficiency (%)
1	20	1	340.7±15.92	0.35±0.020	-20.50±0.37	66.43±11.23
2	20	2	306.1±10.00	0.36±0.050	-29.30±0.88	52.83±7.17
3	20	3	213.87±7.13	0.37±0.010	-27.90±1.20	35.20±3.19
4	20	4	249.53±13.26	0.38±0.040	-32.00±0.36	34.93±2.05
5	40	1	325.50±6.42	0.24±0.020	-30.27±0.41	53.50±1.13
6	40	2	309.53±4.50	0.29±0.020	-20.57±0.59	65.87±1.13
7	40	3	285.90±1.02	0.15±0.010	-27.03±0.48	52.63±7.04
8	40	4	317.67±5.82	0.25±0.010	-28.97±0.24	46.53±5.57
9	80	1	258.43±15.33	0.17±0.010	-21.23±0.81	71.33±7.02
10	80	2	237.63±0.62	0.16±0.003	-27.57±1.44	53.67±1.04
11	80	3	189.53±17.97	0.18±0.008	-20.30±0.22	21.63±3.58
12	80	4	205.73±1.19	0.15±0.007	-26.97±0.81	12.20±0.45

Attenuated total reflectance-Fourier transform infrared spectroscopy (ATR-FTIR)

ATR-FTIR spectrometer provides structural and compositional information of the samples and Spectrum 100 (Perkin Elmer, Massachusetts, USA) was used. The samples were scanned in the range of 600–4000/cm.

In vitro release profile of the fabricated nanoparticles

Nanoparticles (10 mg) were weighed accurately and placed in a tube. A volume of 4 mL of PBS (pH 7.4) was added to the tubes. The tubes were kept undisturbed at 37°C. Then, 200 µL of the solution was taken out from the tubes at the predetermined time points (30 min, 1, 8, and 24 h) and was subjected for quantification using the UV-visible spectrophotometric method. The same amount of fresh phosphate buffer was re-added into the tubes. The measurement was done in triplicate. The cumulative release of drugs and the standard error for each time point was calculated and presented into a graph.^[27]

Preparation and Characterization of Nanoparticle Loaded Gel

Preparation of nanoparticle loaded gel

Four concentrations of polyacrylic acid gel were prepared namely 0.5%, 0.75%, 1.0%, and 1.25%. Polyacrylic acid powder was weighed and dispersed slowly in distilled water. The solution was left overnight until all the polymer fully hydrated. The polyacrylic acid solution was stirred using mechanical overhead stirrer WiseStir HS-30D (Daihan, Seoul, South Korea) at 500 rev/min for 30 min. Propylene glycol (15% w/w) was added into polyacrylic acid solution and the stirring was continued for another 30 min. A few drops of triethanolamine were added to neutralize polyacrylic acid to pH (6.2–7.6) and the transparent gel was formed. The stirring was continued for another 1 h to ensure homogenous gel formation and to remove the air bubble. A sample of 20 mg of AA-PLGA nanoparticles were weighed and mixed with 1 g of polyacrylic acid gel.

Physical appearance of gel formulations

The prepared gel formulations were inspected visually for homogeneity, texture, lump, and colour.^[42]

pH

The measurement was done using a FE 20/EL 20 digital pH meter (Mettler Toledo, Greifensee, Switzerland). Gel (10 g) each formulation was taken in a 25 mL beaker and the pH meter probe was immersed into the sample and the result was recorded. Each formulation was subjected to pH reading thrice.^[42]

Measurement of gel rheology and viscosity

Gel flow behavior determination was done using a Mars rheometer (Haake, Massachusetts, USA). Data analysis was done using Haake Rheo-Win 3.61.0000 software (Haake, Massachusetts, USA). The graph was presented as shear stress (τ) versus shear (γ).^[34] Apparent viscosity was determined at a shear rate of 100 s⁻¹.^[34] The test was repeated in triplicate for each formulation. The selection of correct viscosity of the oral gel formulation is an important parameter for oral mucosa application. The viscosity should be in a range that allows easy application and distribution on oral mucosa as well as enable sufficient retention on the site of application.^[43] However, the optimum viscosity criteria of oral gel formulation are not established.^[44] Thus, Kin Care oral gel's viscosity was made as a reference for the determination of optimal viscosity for topical oral gel. Kin Care is polyacrylic acid based oral gel and was chosen due to the excellent mucoadhesive properties of its formula.^[45]

Spreadability test

The spreadability of formulations was determined by the parallel plate method.^[44] 1 g of the gel was transferred to the center of the glass plate. The second glass of similar size was placed gently on the formulation and 1 kg weight was placed at the center of the plate with care to avoid sliding of the glass plate. The spread diameter was determined after 3 min where no more spreading was expected.^[46] The test was performed in triplicate for each of the formulations.

Adhesion study

Adhesiveness of gel formulations was measured by the agar plate method.^[44,47] An agar plate of 5 cm diameter was prepared. A circle with 1 cm in diameter was made on the center of the agar plate. Accurately weighed 1 g of gel formulation was placed on the center of the agar plate. The agar plate was slanted at 30° angle for 1 h. The longest distance moved by the sample was measured under room temperature. The test was performed thrice for each of the formulations.

In vitro drug release

Drug release of polyacrylic acid oral gel was analyzed with a Franz diffusion cell using a cellulose acetate membrane. Cellulose acetate an artificial membrane utilized in permeation studies has been established to mimic animal mucosa tissue.^[48] Accurately weighed 1 g sample was spread over a cellulose acetate membrane. The receptor phase of the cell was filled with PBS pH 7.4 at 37°C ± 0.5°C as a dissolution medium. 100 µL of the receiving phase was collected at 1, 2, 3, 4, 5, and 6 h. Fresh PBS (100 µL) was added to the receptor phase every sampling was done to ensure constant volume was achieved. The absorbance of the sample was measured using a UV-visible spectrophotometer at a wavelength of 266 nm. The released ascorbic acid was calculated from the ascorbic acid standard curve.

In vitro drug release kinetic

Drug release from the oral gel was analyzed as per zero-order, first-order, and Higuchi's kinetic models to investigate the drug release pattern mathematically.^[49,50] The following mathematical equations, namely, equation 2, 3, and 4 were used:

Zero-order kinetic model	$M_0 - Mt = K_0 t$
First-order kinetic model	$\ln M_0 / Mt = K_1 t$
Higuchi model	$Mt = K_H t^{1/2}$

where M_0 and Mt stand for the amount of sample taken at time zero or dissolved at a particular time (t). K_0 , k_1 , and K_H are the release kinetic constants acquired from the linear curves of the zero-order, first-order, and Higuchi model, respectively.

Cell Culture

Cell lines

SCC-25 cell line was cultured in DMEM supplemented with 10% FBS and 100 U/mL penicillin-streptomycin. SCC-25 cell line is a human squamous cell carcinoma cell line derived from the tongue of a 70-year-old male patient (ATCC®CRL-1628). This cancer cell line is grouped as stage III oral cavity cancer.^[51] The cells were maintained in a humidified atmosphere with 5% of CO₂ at a 37°C incubator.

Cytotoxicity evaluation of the nanoparticles

MTT assay was utilized to determine the anti-proliferative effect of the optimized nanoparticles. Approximately 1×10^4 SCC-25 cells/well were seeded in a 96-well microplate. The treatment incubation period was conducted at 24 h. The medium was removed after the treatment incubation period ended. An amount of 100 µL of mixed solution (MTT and

complete growth media was added to each well and followed by another four h of MTT incubation in 5% of CO₂ incubator at 37°C. The solution was removed from each well. Next, an amount of 100 µL of DMSO was added to each well to dissolve the formazan crystal formation and was incubated for 30 min. The cell inhibition study for ascorbic acid was evaluated based on the intensity of colorimetric changes from the amount of formazan crystal dissolved by the DMSO. This colorimetric change was quantified by using Infinite M200 NanoQuant (Tecan, Switzerland) microplate reader with the absorbance taken at 570 nm wavelength against the reference wavelength of 630 nm.^[52]

Morphological changes analysis

Morphological changes analysis was conducted to investigate the cytotoxicity effect of AA-PLGA nanoparticles on oral cancer cells. The morphology of SCC-25 cells treated with 1000 µg/mL of AA-PLGA nanoparticles for 24 h was observed with an inverted microscopy Zeiss (Baden-Wurtemberg, Germany).

Statistical Analysis

The results of the study were demonstrated as an average of triplicate data ± standard deviation. The acceptable significance level is at $P < 0.05$. Analysis of variance compares multiple means, and t-test is for pairwise comparison. Statistical analysis was done using SPSS 21 software (IBM SPSS, Illinois, USA).

RESULTS AND DISCUSSION

Design of Experiment

The outline and experimental results are tabulated in Table 2. The experimental data were analyzed and fitted to a linear model. The regression coefficient of particle size, PDI and encapsulation efficiency was 0.96, 0.94, and 0.91, respectively, reflecting the goodness of fit of this model [Table 3]. Besides that, the predicted R-squared was in reasonable agreement with the adjusted R-squared for all the responses, assuring the reliability of the model for interpolation [Table 3]. The adequate precision for particle size, PDI and encapsulation efficiency was found to be 21.062, 15.850, and 15.750, respectively, suggesting the adequate signal and that the model could be used to navigate the design space [Table 3].^[53] The reason is that an adequate precision measures the signal-to-noise ratio where a ratio of more than 4 is desirable, showing the reliability of the experimental data.^[54,55] Thus, it confirms that the model is strong enough to be used for optimization. 3D graph generated by design of experiment software was utilized to visualize the relation between the independent factors and the response [Figure 2].

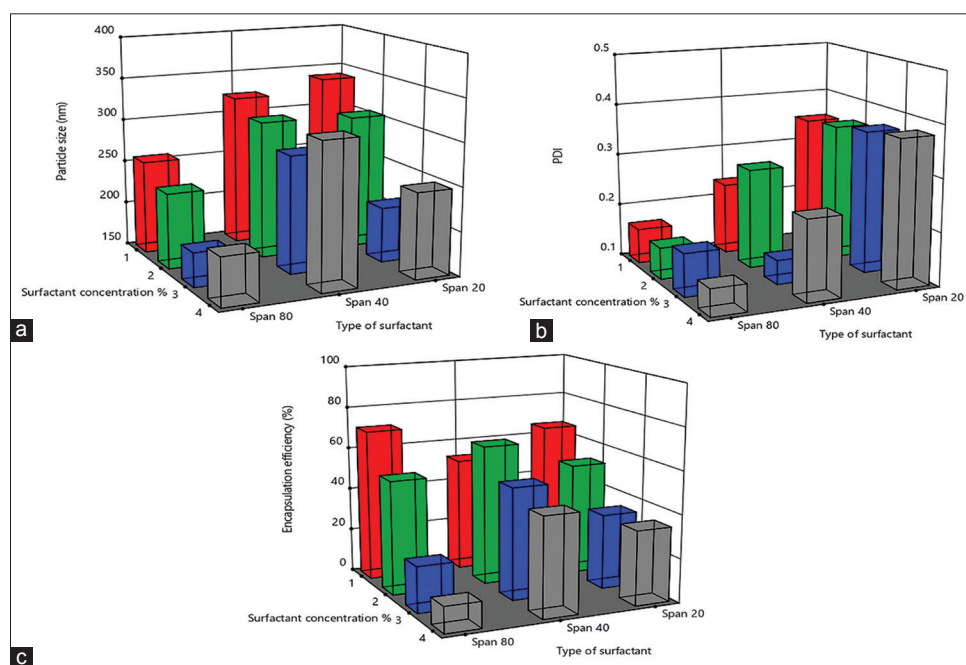
Effect on particle size, PDI and encapsulation efficiency

The particle size of the nanoparticle ranged from 189.53 ± 17.97 nm to 340.7 ± 15.92 nm. The particle size was observed to reduce upon the increase in surfactant concentration [Figure 2a]. This result was in agreement with previous studies that reported a similar trend of particle size reduction and that utilized Span 20 and Span 80 as an emulsifier in the primary emulsion for microparticles and nanoparticles formulations.^[56-60] This effect might be attributed to the role

Table 3: Descriptive statistics of the fitted linear model of particle size, PDI, and encapsulation efficiency. (A) refers to Span surfactant type and (B) refers to surfactant concentration %

Response	Regression model	Regression coefficient (R ²)	Predicted regression coefficient (R _p ²)	Adjusted regression coefficient (Ra ²)	Adequate precision
Particle size	+270.01+7.54A+39.64A ² -10.32B+12.92B ² +5.67B ³ -7.97AB+7.96A ² B+4.65AB ² -0.983A ² B ² +3.61AB ³ -2.52A ² B ³	0.96	0.91	0.94	21.062
PDI	+0.2551+0.1121A-0.0224A ² -0.0004B+0.0026B ² +0.0062B ³ +0.0053AB-0.0044A ² B-0.0021AB ² +0.0107A ² B ² -0.0064AB ³ +0.0166A ² B ³	0.94	0.88	0.92	15.850
Encapsulation efficiency	+47.23+0.1194A+7.4A ² -5.93B+0.2583B ² +1.52B ³ +0.3217AB+4.22A ² B+3.08AB ² -4.88A ² B ² -0.4483AB ³ +0.1183A ² B ³	0.91	0.81	0.88	15.750

PDI: Polydispersity index

**Figure 2:** 3D graph generated by the design expert software to visualize the effect of surfactant type and concentration used in primary emulsion on (a) particle size, (b) polydispersity index (PDI), and (c) encapsulation efficiency

of surfactant as an emulsifier that stabilizes the emulsions by coating the droplets within the system and preventing them from aggregating. Surfactant reduces the interfacial tension and interfacial free energy of two immiscible phases (oil phase and water phase) by aligning themselves at the droplet surface and forming a thin layer around the droplets.^[46] Therefore, the addition of a higher surfactant concentration results in an emulsion with a larger emulsion surface area that produces a smaller particle size.^[38,58] However, this effect was only seen up to 3% concentration of surfactant used for all the surfactant types. Larger particle size was observed with higher surfactant concentration used, such as with 4% of span concentration. This is because the saturation point which also indicates the optimum surfactant concentration has been achieved. A rise in surfactant concentration will not further reduce the size of nanoparticles; instead, it may promote aggregation and increase the particle size.^[61]

The different HLB values of emulsifiers, namely, Span 80 (HLB 4.3), Span 40 (HLB 6.7), and Span 20 (HLB 8.6) were

used for the production of the primary emulsion. Principally, a surfactant contains a hydrophilic head and lipophilic tails.^[25] All Span surfactants possess the same functional group of the hydrophilic head, but a different length of hydrocarbon tail which directly contributes to the HLB value of the surfactant. Thus, a longer hydrophobic tail of the Span surfactant results in a lower HLB value that augments the lipophilicity of the surfactant. The hydrocarbon tail of Span 20 is the shortest followed by Span 40 (longer hydrocarbon tail) and Span 80 (longest hydrocarbon tail). The previous researches have reported that nanoparticles size is proportionate with surfactant HLB value such that the particle size increases as the HLB value increases.^[62,63] It was found that in a W/O, surfactant with a lower HLB value (more lipophilic property) had more reduction in the surface energy and growth of the nucleus, thus leading to a smaller droplet size.^[62] A similar pattern has been shown by Dinarvand *et al.* who studied the effects of different HLB surfactants on naltrexone-loaded PLGA microparticle properties. Formulation using

Span 80 surfactant produced a smaller particle size of the microparticles compared to the microparticles formulated with Span 20, which was in agreement with this current study [Figure 2a]. Thus, according to the hypothesis proposed by the previous finding, the size of the nanoparticles is expected to reduce when the surfactant HLB value decreases in the following order: Span 20 (HLB), Span 40 (HLB), and Span 80 (HLB). From the result, at a 1% concentration of Span surfactant, formulation with Span 20 exhibited the largest nanoparticle size followed by Span 40 and Span 80. However, Span 40 produced a larger size of nanoparticles at a concentration of 2% and above compared to Span 20, contradicting the proposed hypothesis. Both Span 20 and Span 80 have been extensively studied for the formulation of microparticles and nanoparticles.^[56-58,60,64-67] So far, however, there have been few studies regarding the incorporation of Span 40 for nanoparticles formulation. The previous research investigated the effects of Span 40 and Span 80 for nanoparticle formulation through the double emulsification solvent evaporation method. However, the acceptable particle size was only obtained with the addition of Span 80.^[68] In general, it is unlikely that Span 40 is incorporated in the primary emulsion for microparticle and nanoparticle formulation. As shown in the present results, Span 80 with the lowest HLB value (4.3) produced the smallest particle size compared to nanoparticles prepared with other surfactants at all concentrations of surfactant [Figure 2a]. Span 80, which is known as an effective lipophilic surfactant, can efficiently reduce the interfacial tension of W/O compared to higher HLB surfactants. Hence, the smallest droplet size was formed.^[59]

The nanoparticles formulated with Span 20 (0.35–0.38) were observed to exhibit the highest PDI values followed by nanoparticles formulated with Span 40 (0.15–0.29) and Span 80 (0.15–0.18) [Figure 2b]. PDI reflects the distribution of the size population of the nanoparticles, ranging from zero (perfectly uniform size) to one (highly polydisperse size).^[37] A low PDI which is <0.3 is considered monodisperse in the polymeric nanoparticles.^[69,70] Particle size distribution governs the penetration and the accumulation of nanoparticles in the target tissue where only a certain size of nanoparticles would be internalized and retained in the cells. Therefore, the formulation of monodisperse nanoparticles indicated by low PDI values with a certain target size is required to ensure safe, stable and efficient drug delivery to the intended site.^[37] Low PDI values (<0.3) with the incorporation of Span 80 in the primary emulsion of nanoparticles formulation have been reported in the previous studies.^[59,71] The low PDI value obtained with the incorporation of Span 80 may be attributed to its low HLB value. The effective lipophilic surfactant stabilizes the nanodroplets of W/O, resulting in the formation of the narrow size distribution of nanoparticles.^[59]

High drug encapsulation is desired to ensure the efficiency of the nanoparticles system.^[65] In this study, the encapsulation efficiency of AA-PLGA nanoparticles ranged from $12.20 \pm 0.45\%$ to $71.33 \pm 7.02\%$ [Table 2]. The highest encapsulation efficiency (71.33%) was achieved with the incorporation of 1% of Span 80 in the primary emulsion. In brief, surfactant concentration has the opposite impact on encapsulation efficiency, with an increase in surfactant

concentration resulting in a reduction of encapsulation efficiency [Figure 2c]. A similar trend was observed in previous studies.^[56,59,60] Since smaller nanoparticles size was observed with increasing surfactant concentration [Figure 2a], the study proposed that smaller particles of highly surface-active nanoparticles might contribute to a substantial loss of drug during washing compared to larger particles size.^[59] The reason is that a high surface area of smaller nanoparticles further gives an opportunity for the drug to escape.^[58]

Optimization of Nanoparticles and Validation of Model

The desirability function is the most currently used multi-criteria methodology for optimization.^[21] Hence, numerical optimization using the desirability function was applied to obtain the best-optimized nanoparticles formulation. The desirability score ranged between zero to one, and the maximum desirability value indicated that the formulation achieved favorable results for all the responses.^[72] The optimum condition applied for the nanoparticle's optimization was to minimize particle size, PDI <0.3, zeta potential lower than -20 mV and maximized encapsulation efficiency of ascorbic acid. The software recommended three solutions out of 12 combinations of multilevel categorical full-factorial design. Formulation employing 1% Span 80 as the surfactant in primary emulsion exhibited the highest desirability value (0.794), and it was proposed and selected by the software as an optimized formulation. All the formulation responses with 1% Span 80 fell within the desired criteria with the highest ascorbic acid encapsulation efficiency (71.33%). The other three solutions were not selected since the desirability value was low [Table 4]. The recommended solutions for the optimized formulations are presented in Table 4. Validation was performed to confirm the reliability and precision of the model. The second experiment of the optimized formulation was performed and ran in triplicate. The responses of the selected formulation were compared with the predicted values as shown in Table 5. One sample t-test was performed, and the observed experimental values for all the responses were compared with the predicted value suggested by the software. The t-test result showed that no significant difference ($P > 0.05$) was observed between the experimental results and the predicted values for all the responses. Thus, the result assured the validity and precision of the model. The experimental values of the optimized formulation were found in good agreement with the predicted value.

Characterization of Optimized Nanoparticle

Particle size, PDI and zeta potential

The average particle size of the optimized formulation was 252 ± 2.98 nm [Figure 3]. The nanoparticles must be able to penetrate the mucosa barrier and retain in the cancerous epithelium.^[28] Oral mucosa comprises non-keratinized squamous epithelium that is decorated with numerous membrane ridges called microplacae.^[73] The furrow between the microplacae has a diameter of 200–400 nm.^[74] Microplacae were reported to govern the penetration of nanoparticles

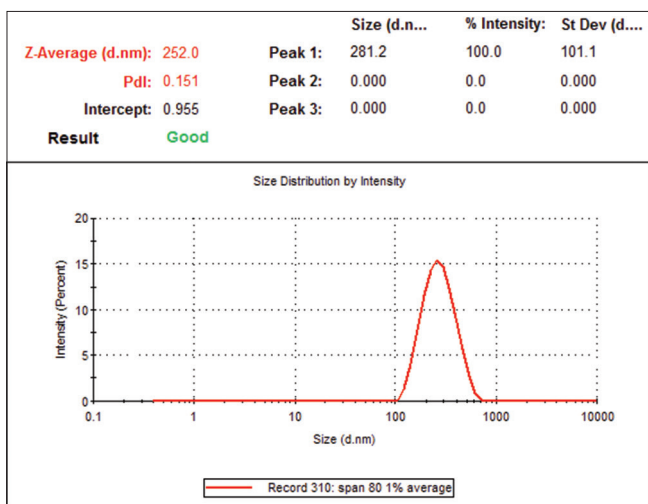
Table 4: Solutions for 12 combinations of categorical factor levels

A	B	Particle size	Polydispersity index	Zeta potential	Encapsulation efficiency	Desirability
Span 80	1	258.433	0.167	-21.233	71.333	0.794
Span 40	2	309.533	0.292	-20.567	65.867	0.400
Span 20	1	340.700	0.353	-20.500	66.433	0.252

Table 5: Validation of the model by comparing the predicted value with the observed experimental value

Response	Predicted value	Mean of the experimental value	P-value
Particle size (nm)	258.43	252.00±2.98	0.067*
Polydispersity index	0.167	0.151±0.02	0.288*
Zeta potential (mV)	-21.2	-20.93±0.87	0.650*
Encapsulation efficiency (%)	71.3	69.73±1.07	0.126*

*P>0.05

**Figure 3:** The Z-average particle size (252.0 nm) and polydispersity index (PDI) (0.151) of the optimized nanoparticles determined by Zetasizer

into the epithelial cells in a size-dependent manner, and the nanoparticles had to be small enough to pass through the furrow.^[74,75] Hence, an optimal particle size is mandatory for efficient cellular uptake.^[76] Correspondingly, a study on the cell penetration by titanium dioxide nanoparticles reported that the nanoparticles were able to penetrate oral mucosa cells in a short time regardless of exposure time and concentration if they were at the right size.^[75] Furthermore, the penetration and retention of fluorescent nanoparticles in the deep layers of the oral epithelium in normal oral mucosa explant and oral cancer cells have been reported in a previous study with fluorescent nanoparticles called FluoSphere having an average particle size of 210 nm.^[28] The acquired particle size from this study seemed to be suitable considering the previously reported size.^[28,77,78] Hence, the developed AA-PLGA is feasible for the local therapy of oral cancer.

The average PDI value of the optimized formulation was 0.151 ± 0.02 [Figure 3]. PDI value of <0.3 was acceptable and monodisperse for the formulation of PLGA-based nanoparticles.^[69,79] The low value of PDI confirmed the narrow distribution of average nanoparticles size. Particle size distribution governs the penetration and the accumulation of nanoparticles in the oral mucosa cells in which only particles that fit the furrow would be internalized and retained in the cells.^[74,75] Therefore, the formulation of monodisperse nanoparticles indicated by low PDI values with a certain range of size is required to ensure safe, stable and efficient drug delivery to the intended site.^[37]

Zeta potential is an indicator of the stability of nanoparticles in dispersion.^[46] Zeta potential lower than -20 mV or higher than $+20$ mV provides acceptable system's stability.^[80,81] The average zeta potential of the optimized nanoparticles was -20.93 ± 0.87 mV [Figure 4]. This finding was consistent with the hypothesis that the negative charges of the zeta potential were attributed to the ionized carboxyl terminal group of the PLGA polymer at the surface of the nanoparticle.^[14,58,79]

ATR-FTIR, SEM and in vitro release study

The SEM microphotographs revealed the presence of spherical-shaped nanoparticles [Figure 5]. A previous study reported that spherical nanoparticles were found deeper in oral mucosa epithelium compared to spindle-shaped nanoparticles.^[75] Thus, this characteristic is very desirable in topical oral mucosa drug delivery. However, all the freeze-dried nanoparticles are in agglomerated form. This phenomenon is commonly observed in nanoscale materials due to the strong Van der Waals attraction that exists between the particles.^[82,83] Hence, it is required to sonicate or sieve the mixture to break down the agglomeration.

The interactions between ascorbic acid and PLGA polymer were studied using ATR-FTIR spectroscopy. No formation of a new peak was observed in the ATR-FTIR spectra of AA-PLGA nanoparticles [Figure 6]. The specific peaks of the functional groups of the PLGA in AA-PLGA nanoparticles were similar to those visible in the blank PLGA material. Therefore, the study suggests that there is no chemical interaction between the functional groups of ascorbic acid and PLGA material. Successful encapsulation of ascorbic acid in PLGA nanoparticles could be deduced from the absence of all the peaks of ascorbic acid in the FTIR spectra of AA-PLGA nanoparticles.

The turnover rate ranges from 2 to 6 days in the oral mucosa. Therefore, the optimized nanoparticles must release most of the active pharmaceutical ingredients before the major turnover, which is within the 1st day after an application to the cancerous site. Hence, the *in vitro* release study was observed for 24 h.^[84] The AA-PLGA nanoparticles exhibited a biphasic

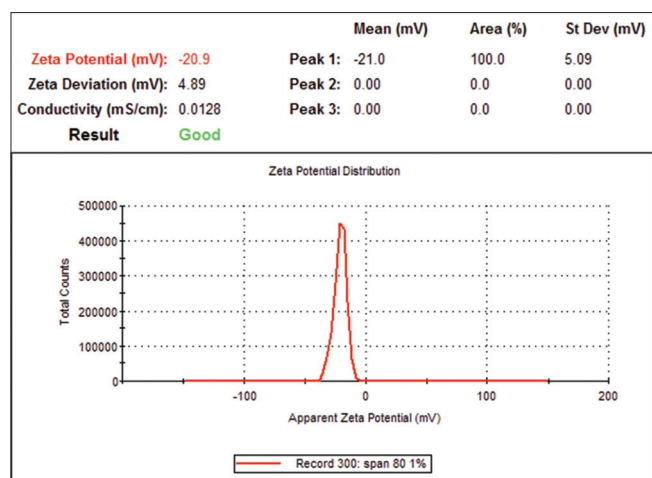


Figure 4: The zeta potential of the optimized AA-PLGA nanoparticles. AA-PLGA: Ascorbic acid-loaded poly(lactic-co-glycolic) acid

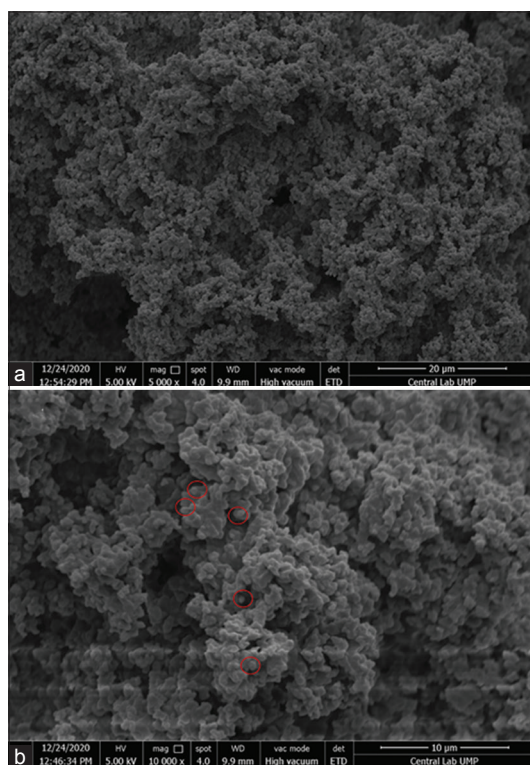


Figure 5: SEM image of the freeze-dried optimized AA-PLGA nanoparticles: (a) at scale of 20 μm and (b) at scale of 10 μm . Red circles indicate the spherical-shaped nanoparticles. AA-PLGA: Ascorbic acid-loaded poly(lactic-co-glycolic) acid

pattern of drug release [Figure 7]. Initial burst release was observed for the first 1 h, followed by slower release later. An amount of $25.98 \pm 8.6\%$ of ascorbic acid was released within 1 h, and $64.88 \pm 0.9\%$ of ascorbic acid was released at 24 h. According to previous studies, the rapid release of ascorbic acid within the first 60 min is attributed to the near-surface entrapped ascorbic acid.^[85,86] Meanwhile, the subsequent slow release is attributed to the remaining ascorbic acid located in the inner part of the PLGA matrix.^[86]

Characterization of Nanoparticles Loaded Gel

Physical appearance of AA-PLGA nanoparticles-in-gel formulation

Before the incorporation of AA-PLGA nanoparticles, the gels were homogeneous in nature, smooth in texture, aggregate-free, transparent, and colorless. Upon the incorporation of AA-PLGA nanoparticles, all the prepared oral gels exhibited white color attributed to the PLGA nanoparticles color [Figure 8].

pH

The pH of all of the prepared formulations was well within the pH range of the oral cavity [Figure 9]. The shift in pH towards acidity has been reported in oral tumors due to anaerobic metabolism of glucose in hypoxic conditions created by the cancer cells. A study found that the average saliva pH of healthy patients was 7.38 while lower pH values of 6.6 and 6.83 were detected in cancer patients without any treatment and after treatment initiation, respectively.^[87] Thus, it can be assumed that the formulated oral gel is applicable for oral mucosa and can be topically applied without the risk of irritation to the oral mucosa.

Flow behavior

All the formulations and the commercial product exhibited non-Newtonian pseudoplastic flow in which the apparent viscosity decreased with increased shear rate [Figure 10]. This property is desirable for oral gel formulation.^[88] Pseudoplastic behavior helps to facilitate the liquid flow out from its container.^[89,90] Good gel flowability is achieved during gel application due to the high shear rate, and viscous gel is formed once applied at the intended site where no pressure is exerted to the gel.^[34]

Viscosity, spreadability and adhesion

The viscosity, spreadability, and adhesion of the prepared oral gels were significantly influenced ($P < 0.001$) by the polyacrylic acid concentration. As the polyacrylic acid concentration increased, the viscosity and adhesion of the gel formulation increased, but the spreadability decreased [Table 6]. An increase of polyacrylic acid concentration results in higher cross-linking between the polymer chains and stronger cohesive forces within a formulation, eventually producing a viscous gel and at the same time, reducing the gel spreading.^[91] Besides that, the movement distance of the gels was used to determine the adhesive property of the formulations on the agar plate.^[44,47] Principally, a shorter movement distance of gel indicates better adhesion between the gel and the agar plate.^[44] The adhesion property is directly related to the polymer concentration; increasing the adhesive polymer will provide better adhesion and hence, prolong the gel residence time. F3 (1% polyacrylic acid) was chosen as the optimum AA-PLGA nanoparticle-loaded gel formulation. F3 (1% polyacrylic acid) exhibited slightly more viscous ($P < 0.05$) gel compared to the reference product; however, the result of the spreadability and adhesion studies was comparable ($p > 0.05$) with the commercial product.

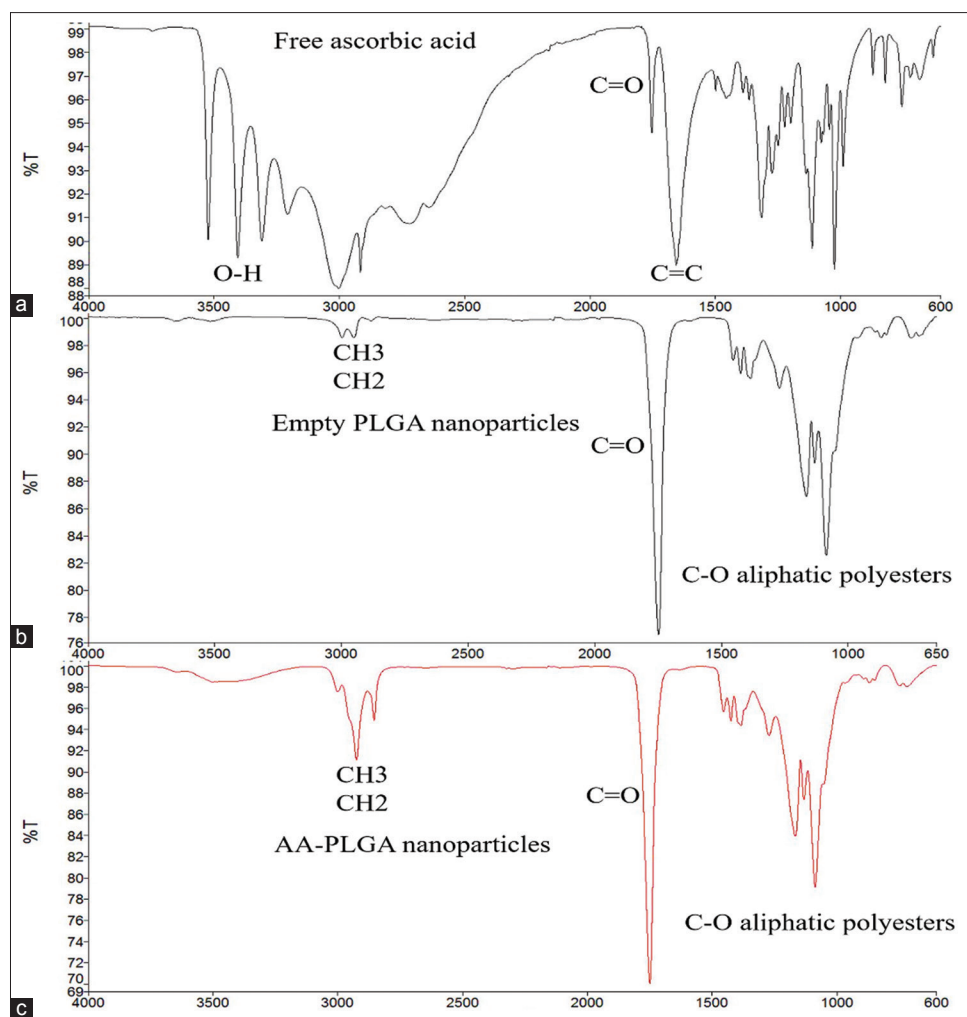


Figure 6: ATR-FTIR spectrum of (a) free ascorbic acid powder, (b) empty PLGA nanoparticles and (c) AA-PLGA nanoparticles. PLGA: Poly(lactic-co-glycolic) acid, AA-PLGA: Ascorbic acid-loaded poly(lactic-co-glycolic) acid

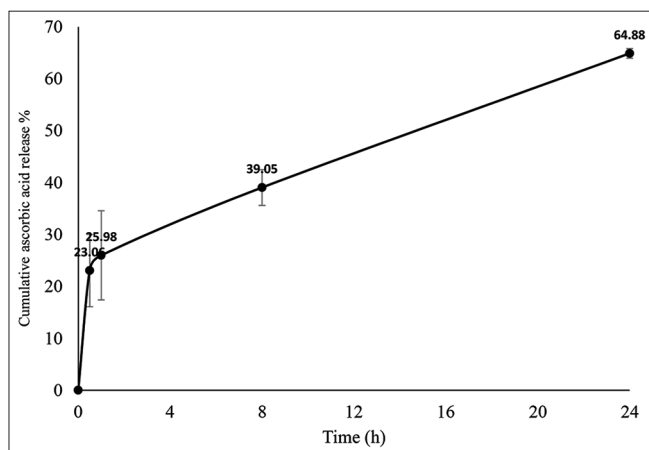


Figure 7: *In vitro* release of ascorbic acid from PLGA nanoparticles in PBS (pH 7.4) at 37°C. Results are given as mean ($n=3$). PLGA: Poly(lactic-co-glycolic) acid

In vitro release study

The maximum duration of oral mucosa delivery is approximately around 4–6 h.^[92] Hence, the *in vitro* release

profile was conducted for 6 h.^[42,93] The release profile of encapsulated ascorbic acid from 1% polyacrylic acid oral gel is shown in Figure 11. It was observed that the total amount of ascorbic acid release at 6 h was $42.91 \pm 4.3\%$ ($4.2 \text{ mg} \pm 0.43 \text{ mg}$). Data from *in vitro* were fitted into the different mathematical models. The data from F3 formulation (1% polyacrylic acid) fitted well to the zero-order kinetics ($R^2 = 0.9771$), suggesting that the system released the drug at a constant rate for 6-h duration [Table 7]. This release kinetic is favorable because the ascorbic acid is released in a controlled manner at a constant rate for 6 h.^[50,94] This finding was consistent with several previous studies that used polyacrylic acid as their major release-controlling polymer.^[49,50,94]

Cytotoxicity Evaluation on Oral Cancer SCC-25 Cell Line

The SCC-25 cell line exhibited a reduction of cell viability percentage in a dose-dependent manner after 24 h incubation with several concentrations of AA-PLGA nanoparticles. The cell viability percentage of SCC-25 cell line after treatment with 200 $\mu\text{g/mL}$, 600 $\mu\text{g/mL}$, 1000 $\mu\text{g/mL}$ and 3600 $\mu\text{g/mL}$ of

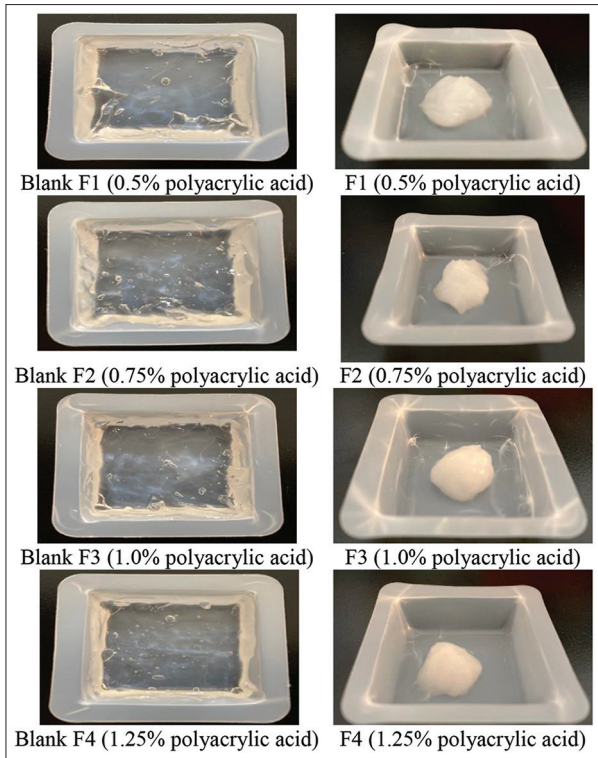


Figure 8: The physical appearance of blank gel and ascorbic AA-PLGA nanoparticles-in-gel formulation with different concentrations of polyacrylic acid polymer. AA-PLGA: Ascorbic acid-loaded poly(lactic-co-glycolic) acid

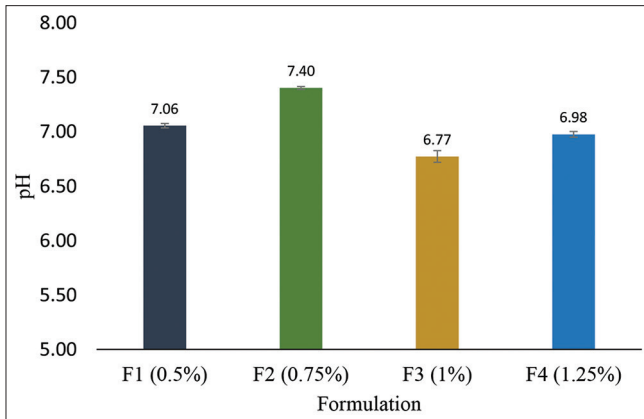


Figure 9: Gel pH

AA-PLGA nanoparticles was $92.14 \pm 3.14\%$, $83.93 \pm 5.78\%$, $67.89 \pm 8.84\%$, and $30.77 \pm 2.11\%$, respectively [Figure 12a]. Statistical analysis showed that significant cytotoxic effects ($P < 0.05$) were reported with $600 \mu\text{g/mL}$, $1000 \mu\text{g/mL}$ and $3600 \mu\text{g/mL}$ of AA-PLGA nanoparticles compared to untreated cells. The half-maximal inhibitory concentration of AA-PLGA nanoparticles calculated through the equation of $y = mx + c$ was $2420 \mu\text{g/mL}$. Besides that, this concentration is also remarkably safe since a high dose of intravenous ascorbic acid is known to have a good safety profile over a broad range of doses namely 1–125 g/day with minor side effects, such as stomach discomfort and headache.^[95-97]

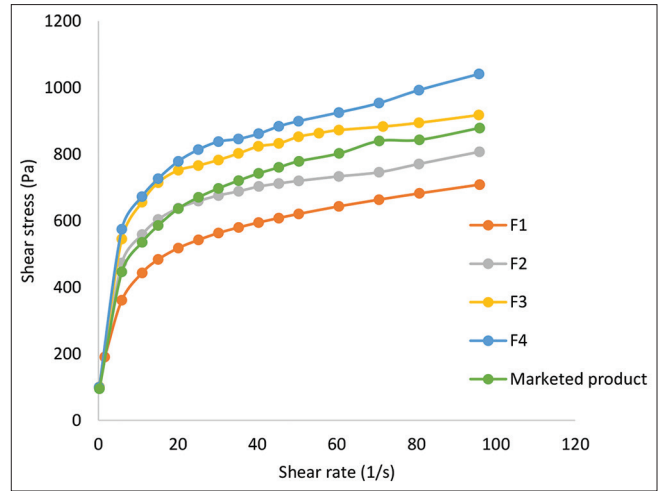


Figure 10: The flow curve of all the gel formulation

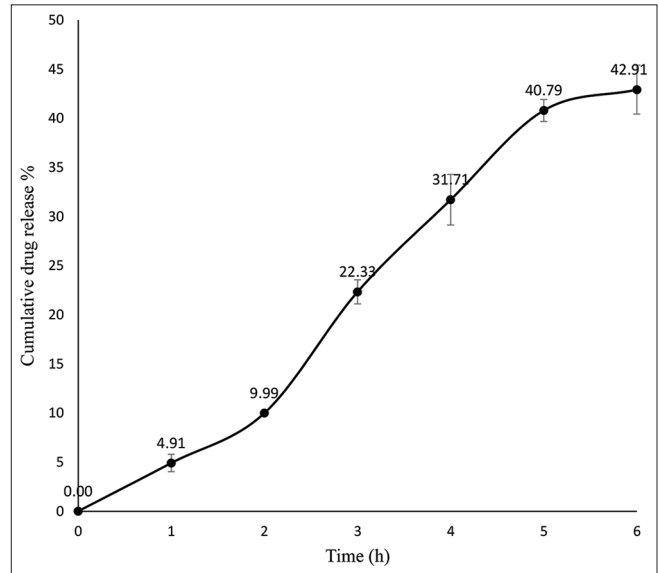


Figure 11: *In vitro* release profile of encapsulated ascorbic acid from 1% polyacrylic acid oral gel at pH 7

Table 6: The characteristic of the prepared gel compared to marketed products

Formulation	Viscosity (Pa.s)	Spreadability (cm)	Adhesion (cm)
F1 (0.5%)	7.130 ± 0.003^a	5.1 ± 0.12^a	2.5 ± 0.40^a
F2 (0.75%)	8.178 ± 0.007^b	4.8 ± 0.05^b	0.5 ± 0.05^b
F3 (1.00%)	9.278 ± 0.152^c	4.3 ± 0.05^c	0.3 ± 0.05^b
F4 (1.25%)	10.520 ± 0.004^d	3.9 ± 0.03^d	0.2 ± 0.05^c
KinCare gel	8.796 ± 0.002^e	4.4 ± 0.05^c	0.4 ± 0.05^b

All analysis is the mean of triplicate reading \pm standard deviation. Means not sharing the same letter in the same column were significantly different at $P < 0.05$. Letters 'a' to 'e' indicate the statistically significant of the result between the formulations

The expected underlying mechanism of the anticancer effect of ascorbic acid is through the pro-oxidant effect. The millimolar concentration of ascorbic acid is able to reduce the transition metal ions such as ferric and cupric cations that are

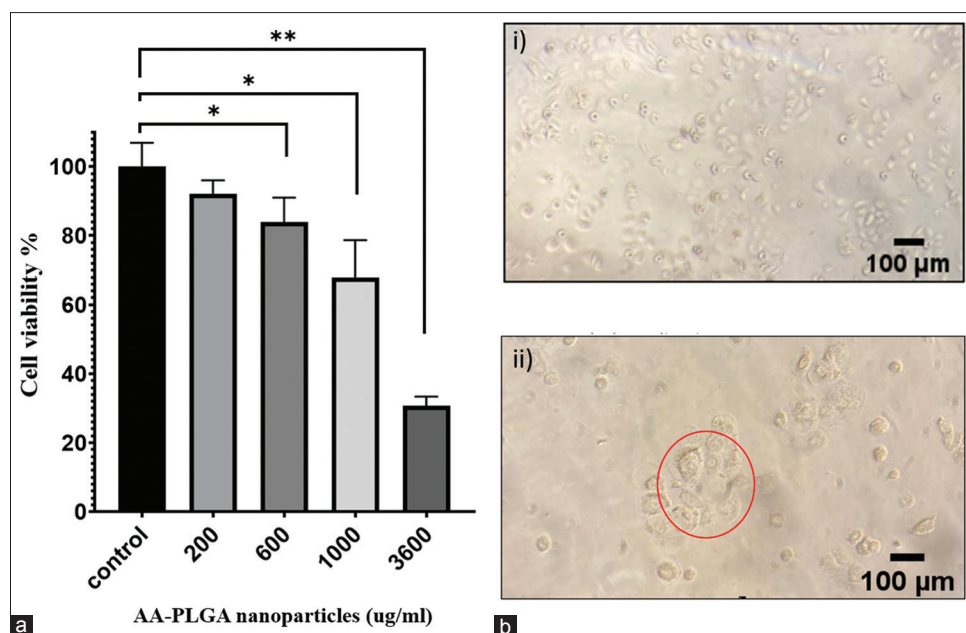


Figure 12: Cytotoxicity result of optimized nanoparticles against SCC-25. (a) Cell viability percentage of SCC-25 cell line after treatment with AA-PLGA nanoparticles for 24 h. Data presented as mean \pm SD. * $P < 0.05$ and ** $P < 0.001$ indicate a significant difference between control (untreated) and treated group. (b) Microscopic appearance of SCC-25 cell line: (i) Untreated SCC-25 cell line and (ii) SCC-25 cell line incubated with 1000 $\mu\text{g}/\text{mL}$ of AA-PLGA nanoparticles. The red circles showed severe morphological alteration which indicated cell death. The images were taken at a magnification of $\times 100$. AA-PLGA: Ascorbic acid-loaded poly(lactic-co-glycolic) acid

Table 7: *In vitro* release kinetic study of topical AA-PLGA oral gel with 1% polyacrylic acid

Zero-order (R^2)	First-order (R^2)	Higuchi (R^2)	Best fitted model
0.9771	0.9726	0.8630	Zero-order

AA-PLGA: Ascorbic acid-loaded poly (lactic-co-glycolic) acid

present in cell culture media. The reduced metal ion further generates reactive oxygen species (ROS) and free radicals through the reduction of oxygen to superoxide radicals which react with themselves and form hydrogen peroxide in the cancer cells.^[97] The formation of a high amount of hydrogen peroxide would cause oxidative stress in cancer cells, leading to the arrest of tumor cell growth and the induction of cancer cell death.^[9,98] This effect was studied in various cancer types including oral cancer cells. A remarkable increment of intracellular ROS levels was evidenced in the HSC-4 cell line, Hep2 cell line and SCC-9 cell line after the exposure to the millimolar concentration of ascorbic acid.^[7-9] Furthermore, it is suggested that the cytotoxic effect of a high concentration of ascorbic acid is cancer-selective due to the differences in catalase activity in cancerous and normal cells. Catalase is known as the enzyme responsible to protect the cell from damage by metabolizing the ROS to safer compounds, namely water and oxygen. A reduced level of ROS metabolizing enzyme has been reported in oral carcinoma patients.^[99-101]

Cellular morphological alteration was also observed after 24 h of cell incubation with 1000 $\mu\text{g}/\text{mL}$ AA-PLGA nanoparticles [Figure 12b]. This finding confirmed the occurrence of cell death after the treatment of encapsulated ascorbic acid. Similarly, abnormal morphological characteristics such as cell deformation, cell shrinkage, and reduction of the total number of cells were

observed in CAL27, SCC-9, and SCC-25 cell lines after 72 h of treatment of 300 $\mu\text{g}/\text{mL}$ and 600 $\mu\text{g}/\text{mL}$ ascorbic acid.^[9]

CONCLUSION

This study successfully developed and characterized AA-PLGA nanoparticles incorporated in polyacrylic acid oral gel. Optimized AA-PLGA nanoparticles were fabricated efficiently through a double emulsion solvent evaporation method. The incorporation of mucoadhesive polymer, namely, polyacrylic acid as oral gel, was able to control the release of drug at a constant rate for an extended duration of time (6 h). The high concentration of AA-PLGA nanoparticles mediated a significant ($P < 0.05$) cytotoxic effect to the human squamous cell carcinoma, SCC-25, in a dose-dependent manner. Thus, AA-PLGA nanoparticles can be regarded as the potential alternative to treat oral cancer.

ACKNOWLEDGMENT

This study was supported by the International Islamic University Malaysia (IIUM) Research under Acculturation Grant Scheme [18-026-0027].

REFERENCES

- Sung H, Ferlay J, Siegel RL, Laversanne M, Soerjomataram I, Jemal A, et al. Global Cancer Statistics 2020: GLOBOCAN estimates of incidence and mortality worldwide for 36 cancers in 185 Countries. *CA Cancer J Clin* 2021;71:209-49.
- Le Champion AC, Ribeiro CM, Luiz RR, da Silva Júnior FF, Barros HC, Dos Santos KC, et al. Low survival rates of oral and oropharyngeal squamous cell carcinoma. *Int J Dent* 2017;2017:5815493.
- Hartner L. Chemotherapy for oral cancer. *Dent Clin North Am*

- 2018;62:87-97.
4. Zhuang Z, Hu F, Hu J, Wang C, Hou J, Yu Z, et al. MicroRNA-218 promotes cisplatin resistance in oral cancer via the PPP2R5A/Wnt signaling pathway. *Oncol Rep* 2017;38:2051-61.
 5. Marcazzan S, Varoni EM, Blanco E, Lodi G, Ferrari M. Nanomedicine, an emerging therapeutic strategy for oral cancer therapy. *Oral Oncol* 2018;76:1-7.
 6. Li S, Wu Y, Ding Y, Yu M, Ai Z. CerS6 regulates cisplatin resistance in oral squamous cell carcinoma by altering mitochondrial fission and autophagy. *J Cell Physiol* 2018;233:9416-25.
 7. Ohwada R, Ozeki Y, Saitoh Y. High-dose ascorbic acid induces carcinostatic effects through hydrogen peroxide and superoxide anion radical generation-induced cell death and growth arrest in human tongue carcinoma cells. *Free Radic Res* 2017;51:684-92.
 8. Baek MW, Cho HS, Kim SH, Kim WJ, Jung JY. Ascorbic acid induces necrosis in human laryngeal squamous cell carcinoma via ROS, PKC, and calcium signaling. *J Cell Physiol* 2017;232:417-25.
 9. Zhou J, Chen C, Chen X, Fei Y, Jiang L, Wang G. Vitamin C promotes apoptosis and cell cycle arrest in oral squamous cell carcinoma. *Front Oncol* 2020;10:976.
 10. Sheraz MA, Khan MF, Ahmed S, Kazi SH, Ahmad I. Stability and stabilization of ascorbic acid. *Househ Pers Care Today* 2015;10:22-5.
 11. Duarah S, Durai RD, Narayanan VB. Nanoparticle-in-gel system for delivery of Vitamin C for topical application. *Drug Deliv Transl Res* 2017;7:750-60.
 12. Kheynoor N, Mohammad S, Hosseini H, Yousefi G, Gahruie HH, Mesbahi G. Encapsulation of Vitamin C in a rebaudioside-sweetened model beverage using water in oil in water double emulsions. *LW Food Sci Technol* 2018;96:419-25.
 13. Hu F, Liu W, Yan L, Kong F, Wei K. Optimization and characterization of poly(lactic-co-glycolic acid) nanoparticles loaded with astaxanthin and evaluation of anti-photodamage effect *in vitro*. *R Soc Open Sci* 2019;6:191184.
 14. Lee SS, Lee YB, Oh JJ. Cellular uptake of poly(dl-lactide-co-glycolide) nanoparticles: Effects of drugs and surface characteristics of nanoparticles. *J Pharm Investig* 2015;45:659-67.
 15. Blasi P. Poly(lactic acid)/poly(lactic-co-glycolic acid)-based microparticles: An overview. *J Pharm Investig* 2019;49:337-46.
 16. Thakur S, Pramod K, Malviya R. Utilization of polymeric nanoparticle in cancer treatment: A review. *J Pharm Care Health Syst* 2017;4:1000172.
 17. Chen G, Wen J. Poly(lactic-co-glycolic acid) based double emulsion nanoparticle as a carrier system to deliver glutathione sublingually. *J Biomed* 2018;3:50-9.
 18. Öztürk AA, Namlı İ, Güleç K, Kıyan HT. Diclofenac sodium loaded PLGA nanoparticles for inflammatory diseases with high anti-inflammatory properties at low dose: Formulation, characterization and *in vivo* HET-CAM analysis. *Microvasc Res* 2020;130:103991.
 19. Ismail R, Sovány T, Gácsi A, Ambrus R, Katona G, Imre N, et al. Synthesis and statistical optimization of Poly (Lactic-Co-Glycolic Acid) nanoparticles encapsulating GLP1 analog designed for oral delivery. *Pharm Res* 2019;36:99.
 20. Rajasree PH, Paul W, Sharma CP, Osmani RA, Hani U, Srivastava A. Eudragit encapsulated cationic poly (lactic-co-glycolic acid) nanoparticles in targeted delivery of capecitabine for augmented colon carcinoma therapy. *J Drug Deliv Sci Technol* 2018;46:302-11.
 21. Sarkar P, Bhattacharya S, Pal TK. Application of statistical design to evaluate critical process parameters and optimize formulation technique of polymeric nanoparticles. *R Soc Open Sci* 2019;6:190896.
 22. Iqbal M, Zafar N, Fessi H, Elaissari A. Double emulsion solvent evaporation techniques used for drug encapsulation. *Int J Pharm* 2015;496:173-90.
 23. Urbaniak T, Musiał W. Influence of solvent evaporation technique parameters on diameter of submicron lamivudine-poly-ε-caprolactone conjugate particles. *Nanomaterials* 2019;9:1240-57.
 24. Khan BA, Akhtar N, Khan HM, Waseem K, Mahmood T, Rasul A, et al. Basics of pharmaceutical emulsions: A review. *African J Pharm Pharmacol* 2011;5:2715-25.
 25. Miller R. Emulsifiers: Types and uses. In: *Encyclopedia of Food and Health*. 1st ed. Netherlands: Elsevier Ltd.; 2015. p. 498-502.
 26. Ketabat F, Pundir M, Mohabatpour F, Lobanova L, Koutsopoulos S, Hadjiiski L, et al. Controlled drug delivery systems for oral cancer treatment-current status and future perspectives. *Pharmaceutics* 2019;11:3.
 27. Matos BN, Pereira MN, Bravo MO, Cunha-Filho M, Saldanha-Araújo F, Gratieri T, et al. Chitosan nanoparticles loading oxaliplatin as a mucoadhesive topical treatment of oral tumors: Iontophoresis further enhances drug delivery *ex vivo*. *Int J Biol Macromol* 2020;154:1265-75.
 28. Holpuch AS, Hummel GJ, Tong M, Seghi GA, Pei P, Ma P, et al. Nanoparticles for local drug delivery to the oral mucosa: Proof of principle studies. *Pharm Res* 2010;27:1224-36.
 29. Desai KG. Polymeric drug delivery systems for intraoral site-specific chemoprevention of oral cancer. *J Biomed Mater Res B Appl Biomater* 2018;106:1383-413.
 30. Sarma H, Jahan T, Sharma HK. Progress in drug and formulation development for the chemoprevention of oral squamous cell carcinoma: A review. *Recent Pat Drug Deliv Formul* 2019;13:16-36.
 31. Hua S. Advances in nanoparticulate drug delivery approaches for sublingual and buccal administration. *Front Pharmacol* 2019;10:1328.
 32. Karthick RA, Devi DR, Hari BN. Investigation of sustained release mucoadhesive *in-situ* gel system of Secnidazole for the persistent treatment of vaginal infections. *J Drug Deliv Sci Technol* 2018;43:362-8.
 33. Sheshala R, Ming NJ, Kok YY, Singh TR, Dua K. Formulation and characterization of pH induced *in situ* gels containing sulfacetamide sodium for ocular drug delivery: A combination of Carbopol®/HPMC polymer. *Indian J Pharm Educ Res* 2019;53:654-62.
 34. Rahman MN, Qader OA, Sukmasari S, Ismail AF, Doolaanea AA. Rheological characterization of different gelling polymers for dental gel formulation. *J Pharm Sci Res* 2017;9:2633-40.
 35. Suzilla WY, Izzati A, Isha I, Zalina A, Rajaletchmy VK. Formulation and evaluation of antimicrobial herbosomal gel from *Quercus infectoria* extract. *IOP Conf Ser Mater Sci Eng* 2020;736:22030.
 36. Bera K, Mazumder B, Khanam J. Study of the mucoadhesive potential of carbopol polymer in the preparation of microbeads containing the antidiabetic drug glipizide. *AAPS Pharm Sci Tech* 2016;17:743-56.
 37. Danaei M, Dehghankhold M, Ateai S, Hasanzadeh Davarani F, Javanmard R, Dokhani A, et al. Impact of particle size and polydispersity index on the clinical applications of lipidic nanocarrier systems. *Pharmaceutics* 2018;10:57.
 38. Nair KG, Velmurugan R, Sukumaran SK. Formulation and optimization of ansamycin-loaded polymeric nanoparticles using response surface methodology for bacterial meningitis. *Bionanoscience* 2020;10:279-91.
 39. Mirakabad FS, Nejati-Koshki K, Akbarzadeh A, Yamchi MR, Milani M, Zarghami N, et al. PLGA-based nanoparticles as cancer drug delivery systems. *Asian Pac J Cancer Prev* 2014;15:517-35.
 40. European Medicine Agency. ICH topic Q2 (R1) Validation of Analytical Procedures: Text and Methodology. Netherlands: European Medicine Agency; 1995.
 41. Maksimenko O, Malinovskaya J, Shipulo E, Osipova N, Razzhivina V, Arantseva D, et al. Doxorubicin-loaded PLGA nanoparticles for the chemotherapy of glioblastoma: Towards the pharmaceutical development. *Int J Pharm* 2019;572:118733.

42. Ahmed AB, Bhaduri I. Development and evaluation of assam bora rice starch-carbopol based oral mucoadhesive gel of irinotecan for mouth cancer. *J Pharm Sci Res* 2017;9:1139-46.
43. Wróblewska M, Szymanska E, Szekalska M, Winnicka K. Different types of gel carriers as metronidazole delivery systems to the oral mucosa. *Polymers (Basel)* 2020;12:680.
44. Kassab HJ, Thomas LM, Jabir SA. Development and physical characterization of a periodontal bioadhesive gel of gatifloxacin. *Int J Appl Pharm* 2017;9:31-6.
45. Laboratories Kin. *Kin Care Oral Gel*. no Date. El Salvador: Laboratories Kin; 2022.
46. Kapileshwari GR, Barve AR, Kumar L, Bhide PJ, Joshi M, Shirodkar RK. Novel drug delivery system of antifungal drug-formulation and characterisation. *J Drug Deliv Sci Technol* 2020;55:101302.
47. Attia MA, El Badawy HY. Film forming gel for treatment of oral mucositis: *In vitro* studies. *Int J Drug Deliv* 2010;2:314-21.
48. Brako F, Thorogate R, Mahalingam S, Raimi-Abraham B, Craig DQ, Edirisinghe M. Mucoadhesion of progesterone-loaded drug delivery nanofiber constructs. *ACS Appl Mater Interfaces* 2018;10:13381-9.
49. Manaswitha A, Sai Swetha PV, Devi NK, Babu KN, Shankar KR. Oleic acid based emulgel for topical delivery of ofloxacin. *J Drug Deliv Ther* 2019;9:183-90.
50. Öztürk AA, Güven UM, Yenilmez E. Flurbiprofen loaded gel based topical delivery system: Formulation and *in vitro* characterization with new developed UPLC method. *Acta Pharm Sci* 2018;56:81-105.
51. Kim K, Lee DJ. The updated AJCC/TNM staging system (8th edition) for oral tongue cancer. *Transl Cancer Res* 2019;8:S164-6.
52. Gupta P, Singh M, Kumar R, Belz J, Shanker R, Dwivedi PD, et al. Synthesis and *in vitro* studies of PLGA-DTX nanoconjugate as potential drug delivery vehicle for oral cancer. *Int J Nanomedicine* 2018;13:67-9.
53. Vakilinezhad MA, Amini A, Dara T, Alipour S. Methotrexate and Curcumin co-encapsulated PLGA nanoparticles as a potential breast cancer therapeutic system: *In vitro* and *in vivo* evaluation. *Colloids Surf B Biointerfaces* 2019;184:110515.
54. Mirahsani A, Sartaj M, Giorgi JB. Assessment and optimization of total ammonia nitrogen adsorption in aqueous phase by sodium functionalized graphene oxide using response surface methodology. *Environ Prog Sustain Energy* 2020;39:1-10.
55. Tay CC, Khoshar-Khan MI, Md-Desa NS, Ab-Ghani Z, Abdul-Talib S. Sustainable optimization of spent mushroom compost activated carbon preparation method using central composite rotatable design response surface methodology. *J Eng Sci Technol* 2015;10:40-51.
56. Mahboubian A, Hashemein SK, Moghadam S, Atyabi F, Dinarvand R. Preparation and *in-vitro* evaluation of controlled release PLGA microparticles containing triptoreline. *Iran J Pharm Res* 2010;9:369-78.
57. Güncüm E, Işıklı N, Anlaş C, Ünal N, Bulut E, Bakırel T. Development and characterization of polymeric-based nanoparticles for sustained release of amoxicillin-an antimicrobial drug. *Artif Cells Nanomed Biotechnol* 2018;46:964-73.
58. Srikar G, Rani AP. Study on influence of polymer and surfactant on *in vitro* performance of biodegradable aqueous-core nanocapsules of tenofovir disoproxil fumarate by response surface methodology. *Braz J Pharm Sci* 2019;55:18736-46.
59. Sayantan R, Akhilesh M, Mandal TK, Sa B, Chakraborty J. Optimization of the process parameters for fabrication of polymer coated layered double hydroxide-methotrexate nanohybrid for possible treatment of osteosarcoma. *R Soc Chem* 2015;5:102574-92.
60. Enayati-Fard R, Akbari J, Saeedi M, Morteza-Semnani K, Morad H, Nokhodchi A. Preparation and characterization of atenolol microparticles developed by emulsification and solvent evaporation. *Lat Am J Pharm* 2019;38:1342-9.
61. Youssef NA, Kassem AA, Farid RM, Ismail FA, El-Massik MA, Boraie NA. A novel nasal almotriptan loaded solid lipid nanoparticles in mucoadhesive *in situ* gel formulation for brain targeting: Preparation, characterization and *in vivo* evaluation. *Int J Pharm* 2018;548:609-24.
62. Housaindokht MR, Pour AN. Study the effect of HLB of surfactant on particle size distribution of hematite nanoparticles prepared via the reverse microemulsion. *Solid State Sci* 2012;14:622-5.
63. Nowroozi F, Almasi A, Javidi J, Haeri A, Dadashzadeh S. Effect of surfactant type, cholesterol content and various downsizing methods on the particle size of niosomes. *Iran J Pharm Res* 2018;17:1-11.
64. Dinarvand R, Moghadam SH, Sheikhi A, Atyabi F. Effect of surfactant HLB and different formulation variables on the properties of poly-D,L-lactide microspheres of naltrexone prepared by double emulsion technique. *J Microencapsul* 2005;22:139-51.
65. Bouriche S, Cózar-Bernal MJ, Rezgui F, Rabasco AM, González-Rodríguez ML. Optimization of preparation method by W/O/W emulsion for entrapping metformin hydrochloride into poly (lactic acid) microparticles using Box-Behnken design. *J Drug Deliv Sci Technol* 2019;51:419-29.
66. Khoee S, Yaghoobian M. An investigation into the role of surfactants in controlling particle size of polymeric nanocapsules containing penicillin-G in double emulsion. *Eur J Med Chem* 2009;44:2392-9.
67. Meenu M, Reeta KH, Dinda AK, Kottarath SK, Gupta YK. Evaluation of sodium valproate loaded nanoparticles in acute and chronic pentylenetetrazole induced seizure models. *Epilepsy Res* 2019;158:106219.
68. Taghipour B, Yakhchali M, Haririan I, Tamaddon AM, Samani SM. The effects of technical and compositional variables on the size and release profile of bovine serum albumin from PLGA based particulate systems. *Res Pharm Sci* 2014;9:407-20.
69. Rafiei P, Haddadi A. A robust systematic design: Optimization and preparation of polymeric nanoparticles of PLGA for docetaxel intravenous delivery. *Mater Sci Eng C Mater Biol Appl* 2019;104:109950.
70. Öztürk AA, Banderas LM, Otero MD, Şenel B, Yazan Y. Dextropropofol trometamol-loaded poly-lactic-co-glycolic acid (PLGA) nanoparticles: Preparation, *in vitro* characterization and cytotoxicity. *Trop J Pharm Res* January 2019;18:1-11.
71. Bazylńska U, Wawrzyńczyk D, Szewczyk A, Kulbacka J. Engineering and biological assessment of double core nanopatform for co-delivery of hybrid fluorophores to human melanoma. *J Inorg Biochem* 2020;208:111088.
72. Pagano C, Giovagnoli S, Perioli L, Tiralti MC, Ricci M. Development and characterization of mucoadhesive-thermoresponsive gels for the treatment of oral mucosa diseases. *Eur J Pharm Sci* 2020;142:105125.
73. Asikainen P, Sirviö E, Mikkonen JJ, Singh SP, Schulten EA, Ten Bruggenkate CM, et al. Microplacae-specialized surface structure of epithelial cells of wet-surfaced oral mucosa. *Ultrastruct Pathol* 2015;39:299-305.
74. Teubl BJ, Leitinger G, Schneider M, Lehr CM, Fröhlich E, Zimmer A, et al. The buccal mucosa as a route for TiO₂ nanoparticle uptake. *Nanotoxicology* 2015;9:253-61.
75. Konstantinova V, Ibrahim M, Lie SA, Birkeland ES, Neppelberg E, Marthinussen MC, et al. Nano-TiO₂ penetration of oral mucosa: *In vitro* analysis using 3D organotypic human buccal mucosa models. *J Oral Pathol Med* 2017;46:214-22.
76. Teubl BJ, Meindl C, Eitzlmayr A, Zimmer A, Fröhlich E, Roblegg E. *In-vitro* permeability of neutral polystyrene particles via buccal mucosa. *Small* 2013;9:457-66.
77. Kumbham S, Paul M, Bhatt H, Ghosh B, Biswas S. Oleonic

- acid-conjugated poly (D, L-lactide)-based micelles for effective delivery of doxorubicin and combination chemotherapy in oral cancer. *J Mol Liq* 2020; 320:114389.
78. Rençber S, Aydın Köse F, Karavana SY. Dexamethasone loaded PLGA nanoparticles for potential local treatment of oral precancerous lesions. *Pharm Dev Technol* 2020;25:149-58.
 79. Öztürk AA, Yenilmez E, Özarda MG. Clarithromycin-loaded poly (Lactic-co-glycolic Acid) (PLGA) nanoparticles for oral administration: effect of polymer molecular weight and surface modification with chitosan on formulation, nanoparticle characterization and antibacterial effects. *Polymers (Basel)* 2019;11:1632.
 80. Kumar R. Lipid-based nanoparticles for drug-delivery systems. In: *Nanocarriers for Drug Delivery*. Netherlands: Elsevier Inc.; 2019. p. 47-76.
 81. Mourdikoudis S, Pallares RM, Thanh NT. Characterization techniques for nanoparticles: Comparison and complementarity upon studying nanoparticle properties. *Nanoscale* 2018;10:12871-934.
 82. Giorgi F, Coglitore D, Curran JM, Gilliland D, Macko P, Whelan M, et al. The influence of inter-particle forces on diffusion at the nanoscale. *Sci Rep* 2019;9:12689.
 83. Umar S, Sulaiman F, Abdullah N, Mohamad SN. Investigation of the effect of pH adjustment on the stability of nanofluid. *AIP Conf Proc* 2018;2031:020031.
 84. Shtenberg Y, Goldfeder M, Prinz H, Shainsky J, Ghantous Y, Abu El-Naaj I, et al. Mucoadhesive alginate pastes with embedded liposomes for local oral drug delivery. *Int J Biol Macromol* 2018;111:62-9.
 85. Arasoglu T, Derman S, Mansuroglu B. Comparative evaluation of antibacterial activity of caffeic acid phenethyl ester and PLGA nanoparticle formulation by different methods. *Nanotechnology* 2016;27:025103.
 86. Amasya G, Badilli U, Aksu B, Tarimci N. Quality by design case study 1: Design of 5-fluorouracil loaded lipid nanoparticles by the W/O/W double emulsion-Solvent evaporation method. *Eur J Pharm Sci* 2016;84:92-102.
 87. Ramya AS, Uppala D, Majumdar S, Surekha Ch, Deepak KG. Are salivary amylase and pH-Prognostic indicators of cancers? *J Oral Biol Craniofac Res* 2015;5:81-5.
 88. Muniz BV, Baratelli D, Di Carla S, Serpe L, da Silva CB, Guilherme VA, et al. Hybrid Hydrogel composed of polymeric nanocapsules co-loading lidocaine and prilocaine for topical intraoral anesthesia. *Sci Rep* 2018;8:17972.
 89. Szymańska E, Orłowski P, Winnicka K, Tomaszewska E, Baška P, Celichowski G, et al. Multifunctional tannic acid/silver nanoparticle-based mucoadhesive hydrogel for improved local treatment of HSV infection: *In vitro* and *in vivo* studies. *Int J Mol Sci* 2018;19:387.
 90. Salah S, Awad GE, Makhlof AI. Improved vaginal retention and enhanced antifungal activity of miconazole microsponges gel: Formulation development and *in vivo* therapeutic efficacy in rats. *Eur J Pharm Sci* 2018;114:255-66.
 91. Magbool FF, Elnima EI, Shayoub ME, Hamedelniei E. Design, formulation, and evaluation of carbopol 940 and xanthan gum as gel bases for oral local drug delivery for oral mucosal infectious diseases. *Eur J Biomed Pharm Sci* 2018;5:9-21.
 92. Verma S, Kaul M, Rawat A, Saini S. An overview on buccal drug delivery system. *Int J Pharm Sci Res* 2011;2:1303-21.
 93. Marques AC, Rocha AI, Leal P, Estanqueiro M, Lobo JM. Development and characterization of mucoadhesive buccal gels containing lipid nanoparticles of ibuprofen. *Int J Pharm* 2017;533:455-62.
 94. Aiyalu R, Govindarjan A, Ramasamy A. Formulation and evaluation of topical herbal gel for the treatment of arthritis in animal model. *Braz J Pharm Sci* 2016;52:493-507.
 95. Leichtle SW, Sarma AK, Strein M, Yajnik V, Rivet D, Sima A, et al. High-dose intravenous ascorbic acid: Ready for prime time in traumatic brain injury? *Neurocrit Care* 2020;32:333-9.
 96. Drisko JA, Serrano OK, Spruce LR, Chen Q, Levine M. Treatment of pancreatic cancer with intravenous Vitamin C: A case report. *Anticancer Drugs* 2018;29:373-9.
 97. Carr AC, Cook J. Intravenous Vitamin C for cancer therapy-identifying the current gaps in our knowledge. *Front Physiol* 2018;9:1182.
 98. Schoenfeld JD, Sibenaller ZA, Mapuskar KA, Wagner BA, Cramer-Morales KL, Furqan M, et al. O₂-and H₂O₂-mediated disruption of Fe metabolism causes the differential susceptibility of NSCLC and GBM cancer cells to pharmacological ascorbate. *Cancer Cell* 2017;31:487-500.
 99. Babiuch K, Bednarczyk A, Gawlik K, Pawlica-Gosiewska D, Kęsek B, Darczuk D, et al. Evaluation of enzymatic and non-enzymatic antioxidant status and biomarkers of oxidative stress in saliva of patients with oral squamous cell carcinoma and oral leukoplakia: A pilot study. *Acta Odontol Scand* 2019;77:408-18.
 100. Rathan Shetty KS, Kali A, Rachan Shetty KS. Serum total antioxidant capacity in oral carcinoma patients. *Pharmacognosy Res* 2015;7:184-7.
 101. Bhat VS, Nayak KR, Kini S, Bhandary BS, Kumari S, Bhat SP. Assessment of serum antioxidant levels in oral and oropharyngeal carcinoma patients. *Internet J Pathol Lab Med* 2016;2:OA1.